ACS OMEGA

http://pubs.acs.org/journal/acsodf

Article

Facile Synthesis of Diversely Functionalized Peptoids, Spectroscopic Characterization, and DFT-Based Nonlinear Optical Exploration

Odette Concepcion, Akbar Ali,* Muhammad Khalid,* Alexander F. de la Torre, Muhammad Usman Khan, Abdul Rauf Raza, Ghulam Mustafa Kamal, Muhammad Fayyaz ur Rehman, Mohammed Mujahid Alam, Muhammad Imran, Ataualpa Albert Carmo Braga, and Mariano W. Pertino

Cite This: *ACS Omega* 2021, 6, 26016−26025

Read Online

ACCESS | Metrics & More | Article Recommendations | Supporting Information

ABSTRACT: Compounds having nonlinear optical (NLO) characteristics have been proved to have a significant role in many academic and industrial areas; particularly, their leading role in surface interfaces, solid physics, materials, medicine, chemical dynamics, nuclear science, and biophysics is worth mentioning. In the present study, novel peptoids (**1**−**4**) were prepared in good yields via Ugi four-component reaction (Ugi-4CR). In addition to synthetic studies, computational calculations were executed to estimate the molecular electrostatic potential, natural bond orbital (NBO), frontier molecular orbital analysis, and NLO properties. The NBO analysis confirmed the stability of studied systems owing to containing intramolecular hydrogen bonding and hyperconjugative interactions. NLO analysis showed that investigated molecules hold noteworthy NLO response as compared to standard compounds that show potential for technology-related applications.

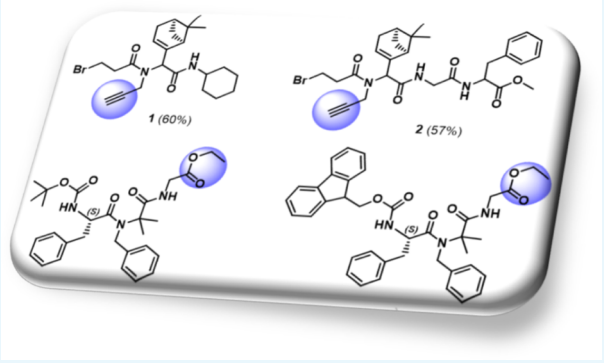

1. INTRODUCTION

Peptoids are significant peptidomimetics with the ability to reveal a widespread array of biological activities, particularly in biomedicine and nanotechnology.[1] The N-substitution of the peptide backbone results in peptoid generation (Figure 1).

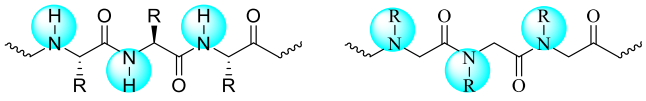

A peptide A peptoid

Figure 1. Structural difference between a peptide and a peptoid backbone.

Ugifour-component reaction is an efficient method to synthesize peptoids of choice for different purposes. This one-pot synthesis using carbonyl, amine, carboxylic acid, and isocyanide moieties is a powerful tool for producing peptoids where enormous diversity can be induced in a single step.[2,3]

The chemical building blocks encompassing NLO properties are extensively investigated for their implementation in optical communication, optical computing, dynamic image processing, and other areas of telecommunication and information technology.[4−6] The theoretical and experimental communities have paid much attention to explore NLO properties of novel systems owing to their blooming applications in surface interfaces, solid physics, materials, medicine, chemical dynamics, nuclear science, and biophysics.[7−11] The literature confirms the organic architectures for exhibiting eminent NLO response.[12−16] Due to supramolecular properties, organic compounds can provide more suitable frameworks than transition-metal organometallic frameworks because of several π-electrons in organic compounds.[17] Since NLO response is generated by the entire electronic structure, complete study of molecular composition is essential to gain insight into NLO response of investigated compounds.[18−20] Both linear and nonlinear responses have vital consideration for appropriate assessment of NLO properties.[21] Therefore, in the current study, we report the synthesis of novel peptoids (**1**−**4**) via Ugi four-component reaction and its NLO behavior exploration through DFT calculations.

Received: June 6, 2021
Published: September 30, 2021

https://doi.org/10.1021/acsomega.1c02962
ACS Omega 2021, 6, 26016−26025

Table 1. E_{HOMO}, E_{LUMO}, and Energy Gap ($E_{LUMO} - E_{HOMO}$) of 1−4 in eV at the DFT/B3LYP/6-311+G (d,p) Level of Theory[a]

	1		2		3		4	
MO(s)	E	ΔE	E	ΔE	E	ΔE	E	ΔE
LUMO	−0.521	6.099	−0.681	5.967	−1.673	4.491	−1.194	4.911
HOMO	−6.620		−6.648		−6.164		−6.105	
LUMO + 1	−0.371	6.491	−0.566	6.381	−0.870	5.631	−0.787	5.944
HOMO − 1	−6.862		−6.947		−6.501		−6.731	
LUMO + 2	−0.238	6.997	−0.468	6.51	−0.595	6.399	−0.594	6.22
HOMO − 2	−7.235		−6.978		−6.994		−6.814	

[a]E = energy, ΔE(eV) = $E_{LUMO} - E_{HOMO}$.

2. COMPUTATIONAL PROCEDURE

GaussView 5.0[22] is utilized for making input files, and the Gaussian 09 program package[23] is employed for exercising computational calculations of novel peptoids (**1**−**4**). At the 6-311+G(d,p) basis set and the B3LYP level of DFT, peptoids (**1**−**4**) were optimized and stability is confirmed via the absence of imaginary frequency. The frontier molecular orbital (FMO), natural bond orbital (NBO), and molecular electrostatic potential (MEP) analyses of investigated compounds **1**−**4** were estimated using the same functional. NLO properties of **1**−**4** were calculated with meta-hybrid GGA M062X, M06 methods, range-corrected CAM-B3LYP, LC-BLYP methods, the exchange correlation B3LYP functional, and the HF method with the 6-311+G(d,p) basis set. Avogadro,[24] Chemcraft,[25] and GaussView 5.0[22] are utilized for fetching the results from output data.

3. RESULTS AND DISCUSSION

3.1. FMO Analysis. FMO analysis is mostly used to explain different properties like reactivity, molecular interactions, electronic features, chemical stability, and charge transfer in different compounds.[26−28] Various chemists and physicists have exercised FMO investigation to expose the structural and geometrical characteristics of investigated systems.[29−36] The aptitude of a molecule to donate or accept the charge density is estimated through FMOs (HOMO and LUMO) energies.[37,38] Moreover, the energy gap between HOMO and LUMO (E_g = $E_{LUMO} - E_{HOMO}$) is a key sign for nonlinear optical behavior of a compound and also used to gauge several parameters including chemical reactivity, ionization potential, chemical hardness, and chemical softness. A compound is considered soft, least stable, and highly reactive if it has a narrow HOMO−LUMO energy gap and vice versa.[39,40] FMO results of **1**−**4** are presented in Table 1. The pictographic display containing red (negative) and blue (positive phase) for LUMO and HOMO, respectively, is portrayed in Figure 2.

The lowest and highest ΔE values among **1**−**4** are for compounds **3** and **1**, respectively. The LUMO and HOMO energies for compound **1** are computed as −0.521 and −6.620 eV, respectively, which result in an energy gap value of 6.099 eV. The population of HOMO and LUMO charge densities is indicated in Figure 2, which is found to be mainly on cyclohexane and the bromine unit of compound **1**. The energy gap in compound **2** is observed as 5.967 eV due to the −0.681 and −6.648 eV energy values of LUMO and HOMO, respectively. The ΔE result in compound **2** is measured less than that in **1** but larger than those in other studied compounds **3** and **4**. The concentration of the HOMO charge density in compound **2** is found mainly on cyclohexane and partially on the carbonyl group. Similarly, the side benzene ring and OCH_3 units are the portions where the LUMO charge density of compound **2** is noticed. In compound **4**, the narrow energy gap of 4.911 eV in contrast to compounds **1** and **2** is observed owing to the −1.194 and −6.105 eV LUMO and HOMO energy values, respectively. The Fmoc group in compound **4** is the populated site for the HOMO charge density, while LUMO is concentrated mainly on the carbonyl group-associated portion and partially on the Fmoc group. The smallest ΔE value (4.491 eV) is measured in **3** among all investigated compounds as results of the −1.673 and −6.164 eV energies associated with LUMO and HOMO of compound **3**, respectively. The HOMO in compound **3** is found to be populated mainly on cyclohexane and naphthalene units of compound **3**. However, LUMO is situated partially on cyclohexane and mainly on the carbonyl group of compound **3**. Inclusive, the growing ΔE order is **3** < **4** < **2** < **1**.

3.2. Global Reactivity Descriptors. The E_{HOMO} and E_{LUMO} are auxiliary applied with the aid of eqs 1−7 to gauge the global reactivity parameters of **1**−**4**[41−44]

$$IP = -E_{HOMO} \quad (1)$$

$$EA = -E_{LUMO} \quad (2)$$

$$X = \frac{[IP + EA]}{2} = -\frac{[E_{LUMO} + E_{HOMO}]}{2} \quad (3)$$

$$\eta = \frac{[IP - EA]}{2} = -\frac{[E_{LUMO} - E_{HOMO}]}{2} \quad (4)$$

$$\mu = \frac{E_{HOMO} + E_{LUMO}}{2} \quad (5)$$

$$\sigma = \frac{1}{2\eta} \quad (6)$$

$$\omega = \frac{\mu^2}{2\eta} \quad (7)$$

The results obtained from eqs 1−7 are listed in Table 2.

The results of IP and EA are mentioned in Table 2, which reveals that our compounds of interest **1**−**4** show lower electron affinity in contrast to ionization potential representing lower electron accepting and greater donating nature of **1**−**4**. The lowest ionization potential value of 6.105 eV among all studied compounds is found to be for **4**, indicating its lowest donating capability. Similarly, the lowest electron affinity value is observed to be 0.521 eV for compound **1**. These results are related to the lowest and highest energy gap values of compounds **4** and **1**, respectively. Similarly, the chemical softness value is found to be the lowest of 0.163961 eV in compound **1** because of its uppermost ΔE value among **1**−**4**. Electronegativity is an added important aspect that describes

https://doi.org/10.1021/acsomega.1c02962
ACS Omega 2021, 6, 26016−26025

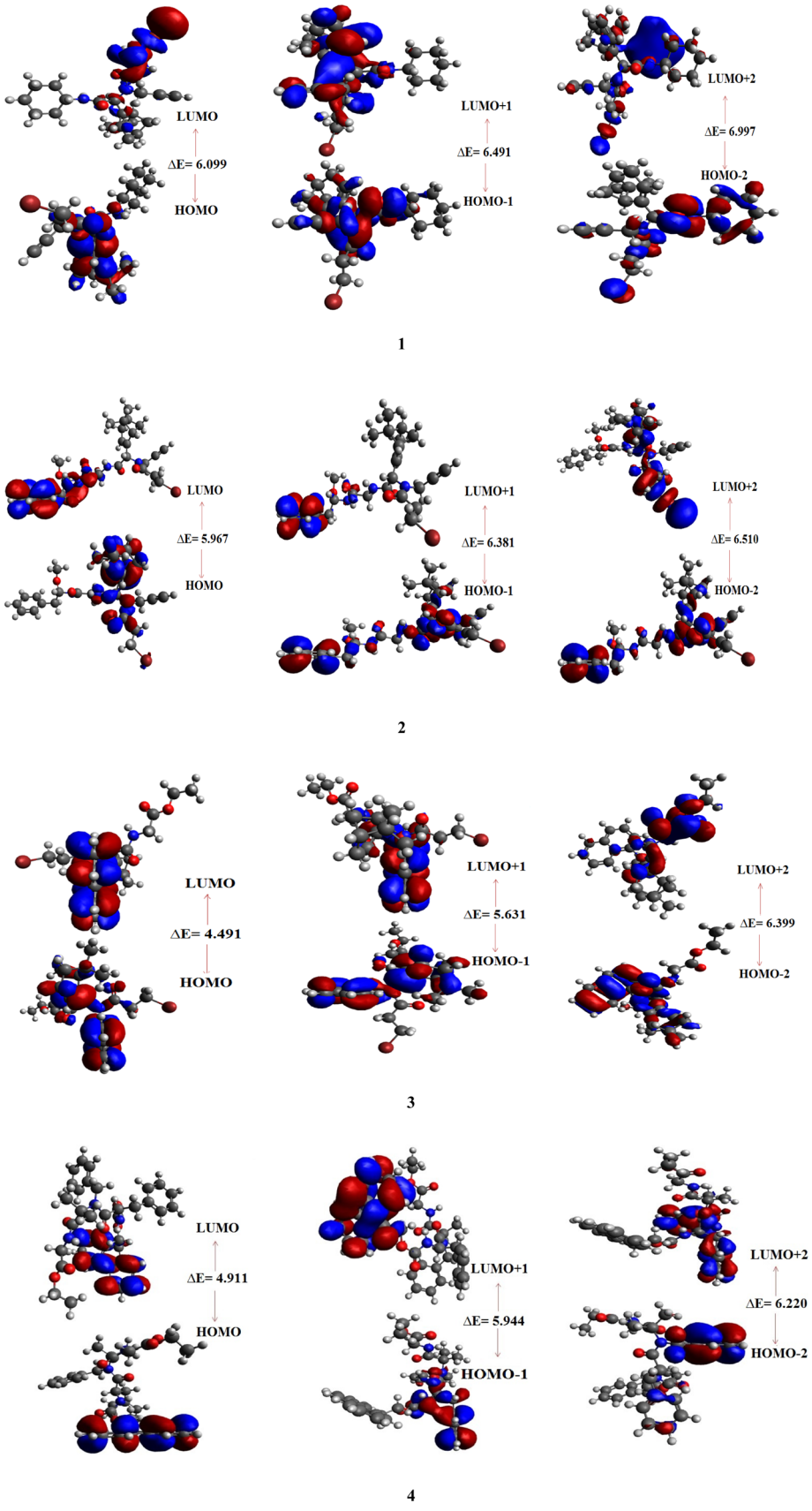

Figure 2. FMOs of investigated compounds **1**−**4**.

the capability to attract charge density. The electronegativity values are measured as **3** > **4** > **2** > **1**. The studied compounds (**1**−**4**) owing to the larger hardness value are recognized as hard, least reactive, and stable. The global hardness value is

https://doi.org/10.1021/acsomega.1c02962
ACS Omega 2021, 6, 26016−26025

Table 2. Ionization Potential (I), Electron Affinity (A), Electronegativity (X), Global Hardness (η), Chemical Potential (μ), Global Electrophilicity (ω), and Global Softness (σ)

compounds	I	A	X	η	μ	ω	σ
1	6.620	0.521	3.5705	3.0495	−3.5705	2.090256	0.163961
2	6.648	0.681	3.6645	2.9835	−3.6645	2.250471	0.167588
3	6.164	1.673	3.9185	2.2455	−3.9185	3.418981	0.222668
4	6.105	1.194	3.6495	2.4555	−3.6495	2.712044	0.203625

Table 3. NBO Analysis of 1−4 by Using the B3LYP/6-311+G (d,p) Functional

	donor (i)	type	acceptor (j)	type	$E(2)^a$ [kcal/mol]	$E(J)E(i)^b$ (a.u)	$F(I,j)^c$ (a.u)
1	$C_{22}-C_{23}$	∂	$C_{23}-H_{55}$	∂^*	0.5	1	0.02
	N_6	LP(1)	C_5-O_9	π^*	69.71	0.27	0.124
	O_{19}	LP(2)	C_2-N_3	∂^*	23.61	0.71	0.117
	O_9	LP(2)	C_4-C_5	∂^*	19.28	0.61	0.098
	N_3	LP(1)	$C_{18}-H_{47}$	∂^*	3.98	0.64	0.049
	$C_{30}-C_{31}$	π	$C_{29}-C_{34}$	π^*	21.13	0.28	0.069
	$C_{29}-C_{34}$	π	$C_{32}-C_{33}$	π^*	20.81	0.28	0.068
	$C_{32}-C_{33}$	π	$C_{29}-C_{34}$	π^*	19.92	0.29	0.068
	$C_{29}-C_{34}$	π	$C_{28}-H_{64}$	∂^*	0.5	0.64	0.018
2	N_6	LP(1)	C_5-O_9	π^*	69.02	0.27	0.123
	N_3	LP(1)	C_2-O_{19}	π^*	62.15	0.27	0.117
	O_{27}	LP(2)	$N_{20}-C_{21}$	∂^*	24.11	0.73	0.12
	N_6	LP(1)	C_7-H_{42}	∂^*	6.52	0.63	0.062
	O_{35}	LP(2)	$C_{26}-H_{62}$	∂^*	3.64	0.69	0.045
	$C_{26}-C_{27}$	π	$C_{18}-C_{28}$	π^*	18.46	0.29	0.066
	$C_{31}-C_{32}$	π	$C_{29}-C_{30}$	π^*	17.38	0.3	0.064
	$C_{18}-C_{28}$	π	$C_{26}-C_{27}$	π^*	16.18	0.3	0.063
	$C_{17}-H_{54}$	∂	$C_{11}-C_{17}$	∂^*	0.50	0.9	0.019
3	N_6	LP(1)	C_5-O_9	π^*	59.43	0.3	0.119
	O_{33}	LP(2)	$C_{20}-O_{23}$	π^*	49.91	0.34	0.116
	O_{23}	LP(2)	$C_{20}-O_{33}$	∂^*	30.69	0.66	0.129
	N_6	LP(1)	C_7-H_{41}	∂^*	6.18	0.64	0.061
	N_6	LP(1)	C_7-H_{40}	∂^*	5.98	0.64	0.06
	N_3	LP(1)	C_4-H_{38}	∂^*	3.39	0.66	0.045
	$C_{25}-C_{33}$	π	$C_{34}-C_{35}$	π^*	30.01	0.25	0.077
	$C_{20}-C_{21}$	π	$C_{22}-C_{23}$	π^*	20.11	0.29	0.068
	$C_{34}-C_{35}$	π	$C_{26}-C_{36}$	π^*	19.84	0.28	0.067
	$C_{87}-H_{88}$	∂	C_5-N_6	∂^*	0.5	0.91	0.019
	N_3	LP(1)	$C_{75}-H_{79}$	∂^*	703.8	0.21	0.376
4	N_3	LP(1)	$C_{24}-C_{32}$	π^*	639.54	0.13	0.264
	O_{38}	LP(2)	$C_{24}-C_{32}$	π^*	440.44	0.02	0.09
	O_{38}	LP(2)	$C_{75}-H_{79}$	∂^*	187.39	0.1	0.126
	O_8	LP(2)	$C_{75}-H_{79}$	∂^*	24.37	0.01	0.015
	N_3	LP(1)	$C_{87}-H_{89}$	∂^*	17.59	2.75	0.214

[a] $E^{(2)}$ means the energy of hyperconjugative interactions (stabilization energy in kcal/mol). [b] Energy difference between donor and acceptor i and j NBO orbitals. [c] $F(i; j)$ is the Fock matrix element between i and j NBO orbitals.

found to be the largest in compound **1** owing to its large energy gap compared to other investigated compounds. The μ has inverse and direct relation with reactivity and chemical stability, respectively. In compounds under our investigation, the chemical potential order is measured as [**3** (μ = −3.9185 eV)] < [**2** (μ = −3.6645 eV)] < [**4** (μ = −3.6495 eV)] < [**1** (μ = −3.5705 eV)]. This order points out that compound **1** has the lowest μ value; hence, it is the least reactive and most stable compound. This result exhibits harmony with ΔE results in which molecules having a larger ΔE value are recognized as small, reactive, and more kinetically stable. Compound **1** is found to be most stable and hard molecule among all investigated molecules. The more donating capability, stability, and least accepting aptitude of **1**−**4** are recommended from inclusive global reactivity parameter conclusions.

3.3. NBO Analysis. The NBO analysis is broadly implemented to explore the various noncovalent and hyperconjugative interactions (HCIs). Hyperconjugative-originated hydrogen bonding (H.B) and transfer of densities from filled to unfilled orbitals are also examined with the help of NBO.[45,46] An attempt is made herein to explore the above-mentioned features in **1**−**4** with the help of eq 8, and the results are listed in Table 3

$$E^2 = q_i \frac{(F_{i,j})^2}{\varepsilon_j - \varepsilon_i} \quad (8)$$

https://doi.org/10.1021/acsomega.1c02962
ACS Omega 2021, 6, 26016−26025

Table 4. Computed Dipole Moments (μ) of Investigated Compounds 1, 2, 3, and 4

compounds	B3LYP	CAM-B3LYP	LC-BLYP	HF	M06	M062X
1	3.8043	3.7432	3.6767	3.7082	3.5128	3.8116
2	5.1890	5.0959	4.9957	4.9461	4.8839	5.1163
3	5.9002	5.8426	5.7849	5.5750	5.6274	5.7579
4	5.6071	5.6613	5.7548	5.5202	5.4517	5.5413

Here, stabilization energy is indicated by E^2; donor orbital occupancy is denoted by q_i; and diagonal elements and off-diagonal NBO elements are represented by ε_j, ε_i, and $F_{i,j}$, respectively.

The $\pi \rightarrow \pi^*$ transitions in compound **1** are found to be least dominant with minute stabilization energy values. This result also confirms the hard nature, stability of compound **1**, and less involvement in charge-transfer reactions. The dominant $\pi \rightarrow \pi^*$ transitions in compound **2** are found to be $\pi(C_{30}-C_{31}) \rightarrow \pi^*(C_{29}-C_{34})$, $\pi(C_{29}-C_{34}) \rightarrow \pi^*(C_{32}-C_{33})$, and $\pi(C_{32}-C_{33}) \rightarrow \pi^*(C_{29}-C_{34})$ with stabilization energy values of 21.13, 20.81, and 19.92 kcal/mol, respectively. In compounds **3** and **4**, $\pi(C_{26}-C_{27}) \rightarrow \pi^*(C_{18}-C_{28})$, $\pi(C_{31}-C_{32}) \rightarrow \pi^*(C_{29}-C_{30})$, $\pi(C_{18}-C_{28}) \rightarrow \pi^*(C_{26}-C_{27})$ and $\pi(C_{25}-C_{33}) \rightarrow \pi^*(C_{34}-C_{35})$, $\pi(C_{20}-C_{21}) \rightarrow \pi^*(C_{22}-C_{23})$, $\pi(C_{34}-C_{35}) \rightarrow \pi^*(C_{26}-C_{36})$ are the dominant $\pi \rightarrow \pi^*$ transitions which stabilized compounds **3** and **4** with energy values of 18.46, 17.38, 16.18 and 30.01, 20.11, 19.84 kcal/mol, respectively. Enormous stabilization energy values are also observed in the case of resonance, which indicated the delocalization of nitrogen and oxygen electrons to the whole molecular unit. These transitions are L.P1(N_6) $\rightarrow \pi^*(C_5-O_9)$, L.P2($O_{19}$) $\rightarrow \pi^*(C_2-N_3)$, L.P2($O_9$) $\rightarrow \pi^*(C_4-C_5)$ with stabilization energies of 69.71, 23.61, 19.28 kcal/mol in **1**; L.P1(N_6) $\rightarrow \pi^*(C_5-O_9)$, L.P1($N_3$) $\rightarrow \pi^*(C_2-O_{19})$, L.P2($O_{27}$) $\rightarrow \pi^*(N_{20}-C_{21})$ with stabilization energies of 69.02, 62.15, 24.11 kcal/mol in **2**; L.P1(N_6) $\rightarrow \pi^*(C_5-O_9)$, L.P2($O_{33}$) $\rightarrow \pi^*(C_{20}-O_{23})$, L.P2($O_{23}$) $\rightarrow \pi^*(C_{20}-O_{33})$ with stabilization energies of 59.43, 49.91, 30.69 kcal/mol in **3**; and L.P1(N_3) $\rightarrow \sigma^*(C_{75}-H_{79})$, L.P1($N_3$) $\rightarrow \pi^*(C_{24}-C_{32})$, L.P2($O_{38}$) $\rightarrow \pi^*(C_{24}-O_{32})$, and L.P2($O_{38}$) $\rightarrow \pi^*(C_{75}-H_{79})$ with stabilization energies of 703.8, 639.54, 440.44, 187.39 kcal/mol in **4**, respectively. NBO results confirm that noncovalent interactions like intramolecular H.B stabilized the donor–acceptor interactions in present investigated systems. The lone pair of L.P1(N3) is delocalized to the anti-bonding sigma orbital of $C_{18}-H_{47}$ and offers 3.98 kcal/mol to compound **1**. Similarly, intramolecular H.B in compound **2** is noted owing to the delocalization of electrons from L.P1(N6) and L.P2(O35) to C_7-H_{42} and $C_{26}-H_{62}$ with energies of 6.52 and 3.64 kcal/mol, respectively. Stabilization energies of 6.18, 5.98, and 3.39 kcal/mol in compound **3** are noted due to delocalization of electrons from L.P1(N_6), L.P1(N_6), and L.P1(N_3) to C_7-H_{41}, C_7-H_{40}, and C_4-H_{38}, respectively. A similar effect is noted in compound **4**, where there is delocalization of electrons from L.P2(O_8), L.P1(N_3), L.P1(N_3), and L.P2(O_{38}) to $C_{75}-H_{79}$, $C_{87}-H_{89}$, $C_{75}-H_{79}$, and $C_{75}-H_{79}$ with stabilization energy values of 24.37, 17.59, 703.8, and 187.39 kcal/mol, respectively.

The $\sigma \rightarrow \sigma^*$ transitions are observed as the least dominant transitions in the investigated molecules. Thus, $\sigma(C_{22}-C_{23}) \rightarrow \sigma^*(C_{23}-H_{55})$, $\sigma(C_{29}-C_{34}) \rightarrow \sigma^*(C_{28}-H_{64})$, $\sigma(C_{17}-H_{54}) \rightarrow \sigma^*(C_{11}-H_{17})$, and $\sigma(C_{87}-H_{88}) \rightarrow \sigma^*(C_5-N_6)$ are the transitions which offer the least stabilization energy value of 0.50 kcal/mol to investigated compounds **1**, **2**, **3**, and **4**, respectively. It is evident from the above discussion that there are successful intramolecular charge transfer, intramolecular H.B, and HCIs among bonds because the electron delocalization on the entire molecule offers stability to the studied **1**, **2**, **3**, and **4** molecules.

3.4. Nonlinear Optical Properties. The expansion of potential communication technology-associated phenomena like enhanced data rates, frequency mixing, and harmonic generation expedited the development of NLO materials and make this area of frontier research. The intramolecular charge transfer (ICT) and wide electronic delocalization in organic compounds extended their utility in the telecommunication sector.[47−51] Consequently, NLO properties of investigated compounds **1**, **2**, **3**, and **4** are measured with combinations of various methods like M062X, M06, CAM-B3LYP, LC-BLYP, B3LYP, and HF with the 6-311+G(d,p) basis set.

Equations 9 and 10 are used to calculate average polarizability and first-order hyperpolarizability (β_{tot}), respectively,

$$\langle a \rangle = 1/3(a_{xx} + a_{yy} + a_{zz}) \tag{9}$$

$$\beta_{total} = [(\beta_{xxx} + \beta_{xyy} + \beta_{xzz})^2 + (\beta_{yyy} + \beta_{yzz} + \beta_{yxx})^2 + (\beta_{zzz} + \beta_{zxx} + \beta_{xyz})^2]^{1/2} \tag{10}$$

The dipole moment results presented in Table 4 indicate that the highest electric dipole moment (μ_{total}) value is found to be 5.9002 D for **3** computed from the B3LYP method, while the lowest μ_{total} value 3.5128 D is measured for **1** calculated from the M06 method among **1**−**4**. The B3LYP method exhibits the uppermost μ_{total} values among **1**, **2**, **3** and **4**. On the other hand, the HF method and meta-hybrid GGA method M06 show lower μ_{total} values than other investigated methods. The overall decreasing order of μ_{total} is **3** > **4** >**2** > **1**.

The exchange correlation functional B3LYP and the M06 method exhibited almost similar values of 301, 377, 372, and 492 with each other for all investigated compounds **1**, **2**, **3**, and **4**, respectively. Furthermore, the highest average polarizability values are also found from B3LYP and M06 methods. On the other hand, the HF method showed minimum average polarizability values of 277.58, 347.2, 343.15, and 455.35 a.u. for **1**, **2**, **3**, and **4**, respectively. Compound **4** among **1**−**4** showed the highest $\langle \alpha_{tot} \rangle$ results with all investigated methods. It is normally considered that compounds with the lowest energy gap exhibited the large polarizability value. This is evidence from these results that the lowest energy gap-valued compound **4** exhibited the highest average polarizability values as compared to other compounds. In contrast, compounds with the highest energy gap value **1** having hard nature revealed the lowermost $\langle \alpha_{tot} \rangle$ results measured from all methods and among all compounds. The increasing order for $\langle \alpha_{tot} \rangle$ with investigated methods is HF < LC-BLYP < M062X < CAM-B3LYP < M06 ≈ B3LYP for **1**, **2**, **3**, and **4**, respectively.

https://doi.org/10.1021/acsomega.1c02962
ACS Omega 2021, 6, 26016−26025

Table 5 confirms that the x-direction tensor (β_{xxx}) and the z-direction tensor (β_{zzz}) contribute the maximum and minimum to β_{tot} values, respectively. The lower β_{tot} values among all methods are shown by the HF method. However, the highest β_{tot} values of 296.02, 421.70, and 451.22 (a.u) are exhibited by the meta-hybrid GGA method M06 in compounds **1**, **2**, and **4**, respectively. However, for **3**, the highest hyperpolarizability value of 555.81 (a.u) is observed from the exchange correlation functional B3LYP method. The investigated method order is noted as M06 > B3LYP > CAM-B3LYP > M062X > LC-BLYP > HF for compound **1**, M06 > B3LYP > CAM-B3LYP > LC-BLYP > M062X > HF for compound **2**, B3LYP > M06>CAM-B3LYP > M062X > LC-BLYP > HF for compound **3**, and M06 > B3LYP > M062X > CAM-B3LYP > HF > LC-BLYP for compound **4**. The urea molecule [β_{tot} (urea) = 69.399 a.u.] was compared with the β_{tot} results of **1**, **2**, **3**, and **4**. Consequently, it had been observed that the highest β_{tot} magnitude of **1**, **2**, **3**, and **4** was observed to be 4.26, 6.07, 8.0, and 6.5 times greater than that of urea, respectively (Table 5). In short, above-mentioned comparative data recommend the excellent NLO features in investigated compounds **1**−**4**.

Table 5. Dipole Polarizabilities and First Hyperpolarizability (β_{Tot}) (a.u) for 1−4

compounds	methods	α_{tot}	β_{tot} (a.u)
1	B3LYP	301.90	253.05
	CAM-B3LYP	294.43	241.69
	LC-BLYP	285.42	224.09
	HF	277.58	218.10
	M06	301.27	296.02
	M062X	294.12	235.68
2	B3LYP	378.23	406.35
	CAM-B3LYP	368.80	379.28
	LC-BLYP	357.37	352.22
	HF	347.21	309.99
	M06	377.72	421.70
	M062X	367.37	340.49
3	B3LYP	372.04	555.81
	CAM-B3LYP	362.79	427.49
	LC-BLYP	351.81	364.96
	HF	343.15	323.68
	M06	372.34	468.47
	M062X	361.27	389.26
4	B3LYP	491.03	303.22
	CAM-B3LYP	479.62	215.43
	LC-BLYP	465.72	186.37
	HF	455.35	200.25
	M06	492.16	451.22
	M062X	476.90	248.23

3.5. MEP Analysis. MEP analysis is used to explain the electrons density in terms of the 3D plot on the entire molecule. The suitable sites for nucleophilic as well as electrophilic attack are described by a band of colors. Blue > green > yellow > orange > red is the decreasing order for electrostatic potential. Blue denotes the positive potential area suitable for nucleophilic attack. However, red describes the negative potential site suitable for electrophilic attack. Figure 3 represents that oxygen and bromine atoms generate the red (negative potential) site, while carbon and hydrogen generate the blue (positive potential) site.

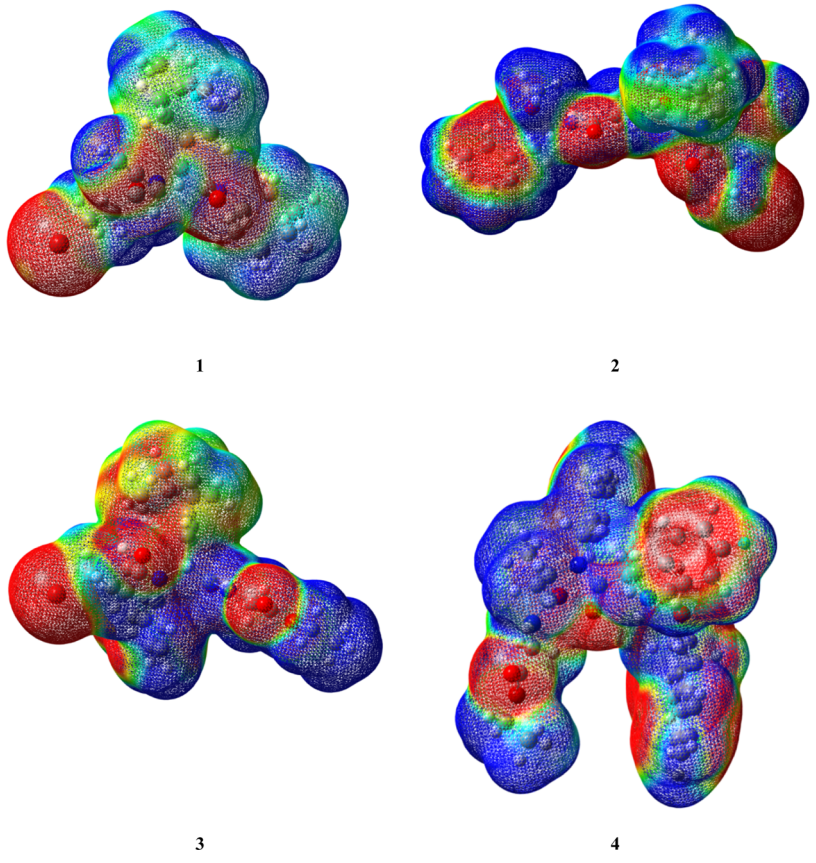

Figure 3. Molecular electrostatic potential of compounds of **1**, **2**, **3**, and **4**.

https://doi.org/10.1021/acsomega.1c02962
ACS Omega 2021, 6, 26016−26025

4. CONCLUSIONS

In conclusion, novel peptoids (**1**−**4**) were synthesized in the isolated yields of 60, 57, 58, and 55%, respectively, using a one-pot multicomponent approach, specifically the Ugi four component reaction (Ugi-4CR), an ecofriendly chemical reaction where the only side product is water. The synthesized peptoid structures were investigated by a spectroscopic technique. Theoretical exploration of the synthesized compounds was achieved using DFT calculations. Accordingly, the FMO analysis confirmed that compound **4** contained the lowest energy gap values, while **1** exhibited the highest energy gap values. The NBO analysis confirmed the presence of intramolecular hydrogen bonding, HCIs that are the pivotal cause for stability of investigated compounds. The more donating capability, stability, and less accepting capability of **1**−**4** are suggested from global reactivity parameter findings. The highest average polarizability and hyperpolarizability values are found from B3LYP and M06 methods. However, the HF method showed minimum average polarizability and hyperpolarizability values. NLO analysis also confirmed that investigated molecules have 4.26, 6.07, 8.0, and 6.5 times higher NLO properties as compared to the prototype standard compound, which disclosed their potential for technology-related applications.

5. EXPERIMENTAL SECTION

5.1. Chemistry. Top grade chemicals were purchased from well-reputed chemical industries like Acrös Chemicals, Sigma-Aldrich, and Fisher Scientific Ltd. and used without further purification for the synthesis of peptoids. Thin-layer chromatography (TLC) was performed via pre-coated silica gel plates to monitor the progress of a reaction. The colorless spots on TLC were visualized by ninhydrin spray or exposure to UV radiation (256 and 365 nm λ). Nuclear magnetic resonance (NMR) spectroscopy (^{1}H, ^{13}C) is used for the structural elucidation of compounds. The ^{1}H and ^{13}C NMR spectra were recorded on 400 and 100 MHz Bruker instruments (AC-400), respectively, at Departamento de Química Orgánica, Facultad de Ciencias Químicas, Universidad de Concepción, Concepción, Chile. The samples were run normally in $CDC1_3$ due to their solubility factor and are referenced to an internal standard (Me_4Si) for ^{1}H spectra.

5.2. General Procedure for the Ugi-4CR. A solution containing carbonyl compounds and amine (1 equiv each) in MeOH was stirred at room temperature for 2 h in order to synthesize the corresponding imine moiety *in situ*. The addition of isocyanide (1 equiv), followed by the addition of carboxylic acid (1 equiv), was carried out to the solution at ambient temperature. The resulting solution was allowed to stir overnight at room temperature. Finally, the solvent was evaporated and the residue was purified by column chromatography using the Et_2O gradient with *n*-hexane.[52−55]

5.2.1. 3-Bromo-N-[cyclohexylcarbamoyl-(6,6-dimethyl-bicyclo[3.1.1]hept-2-ene)-methyl]-N-prop-2-yn-propionamide ***1****.*

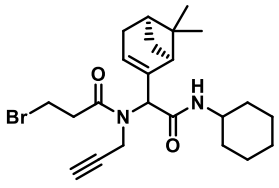

Yield: 60% as a sticky oil; ^{1}H NMR (400 MHz, $CDCl_3$): δ 5.75−5.60 (m, 2H), 5.43−5.24 (m, 1H), 4.27−4.01 (m, 2H), 3.82−3.63 (m, 3H), 3.21−3.07 (m, 1H), 2.40−2.28 (m, 3H), 2.13 (m, 1H), 1.93 (m, 2H), 1.75−1.56 (m, 4H), 1.41−1.25 (m, 7H), 1.23−1.07 (m, 4H), 0.89 (m, 3H). ^{13}C NMR (100 MHz, $CDCl_3$): δ 171.9, 168.1, 142.1, 125.0, 79.6, 72.5, 62.1, 48.4, 44.7, 40.3, 37.9, 37.1, 34.9, 33.0, 32.8, 31.9, 31.6, 26.9, 26.0, 25.5, 24.8, 24.7, 21.1.

5.2.2. Methyl-2-[2-[(3-bromopropionyl)-prop-2-yn-amino]-2-(6,6-dimethyl-bicyclo[3.1.1]hept-2-ene-2)-acetylamino]]-3-phenylpropanoate ***2****.*

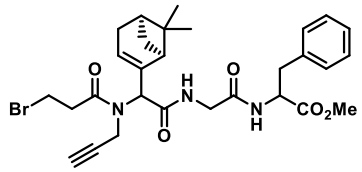

Yield: 57% as a sticky oil; ^{1}H NMR (400 MHz, $CDCl_3$): δ 7.39−7.06 (m, 5H), 6.75−6.46 (m, 1H), 5.76−5.01 (m, 1H), 4.84 (m, 1H), 4.23−3.53 (m, 8H), 3.22−3.05 (m, 2H), 2.51−2.09 (m, 7H), 1.97−1.72 (m, 2H), 1.41−1.20 (m, 6H), 0.95−0.80 (m, 3H). ^{13}C NMR (100 MHz, $CDCl_3$): δ 172.4, 172.0, 169.6, 168.2, 141.2, 135.8, 129.3, 128.6, 127.1, 125.9, 79.2, 72.8, 63.2, 53.3, 52.4, 44.7, 43.0, 40.2, 38.2, 37.7, 37.0, 36.6, 35.1, 31.8, 30.9, 26.7, 26.0, 24.7, 21.0.

5.2.3. Ethyl([2-[benzyl-(2-tert-butoxycarbonylamino-3-phenylpropionyl)amino]-2-methylpropyl amino]ethanoate) ***3****.*

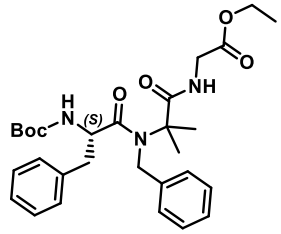

Yield: 58% as a sticky oil; ^{1}H NMR (400 MHz, $CDCl_3$): δ 7.38−7.29 (m, 3H), 7.28−7.21 (m, 5H), 7.03−6.97 (m, 2H), 6.36−6.20 (m, 1H), 5.24−5.12 (m, 1H), 4.61−4.43 (m, 2H), 4.27−4.21 (m, 2H), 4.04 (m, 2H), 3.01−2.74 (m, 2H), 2.33−2.14 (m, 1H), 1.75 (s, 1H), 1.47 (s, 3H), 1.40 (m, 11H), 1.33−1.29 (m, 3H). ^{13}C NMR (101 MHz, $CDCl_3$): δ 174.6, 173.4, 170.3, 155.3, 138.2, 136.7, 129.6, 129.0, 128.4, 127.4, 126.8, 126.2, 79.8, 62.9, 61.4, 53.2, 47.4, 41.7, 39.4, 28.2, 24.1, 14.2.

5.2.4. Ethyl(2-[benzyl-[2-(9H-flouren-9-ylmethoxycarbonylamino)-3-phenyl-propionyl]-amino]-2-methylpropionylamino)ethanoate ***4****.*

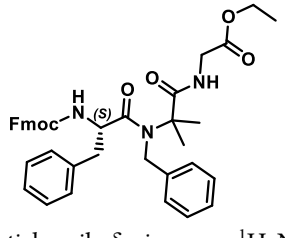

Yield: 55% as a sticky oil; δ_H in ppm: ^{1}H NMR (400 MHz, $CDCl_3$): δ 7.81−7.74 (m, 2H), 7.58 (m, 2H), 7.45−7.30 (m, 6H), 7.27−7.18 (m, 5H), 7.06 (m, 1H), 6.27−6.06 (m, 1H), 5.75−5.52 (m, 1H), 4.71 (m, 1H), 4.51−4.41 (m, 1H), 4.39−

https://doi.org/10.1021/acsomega.1c02962
ACS Omega 2021, 6, 26016−26025

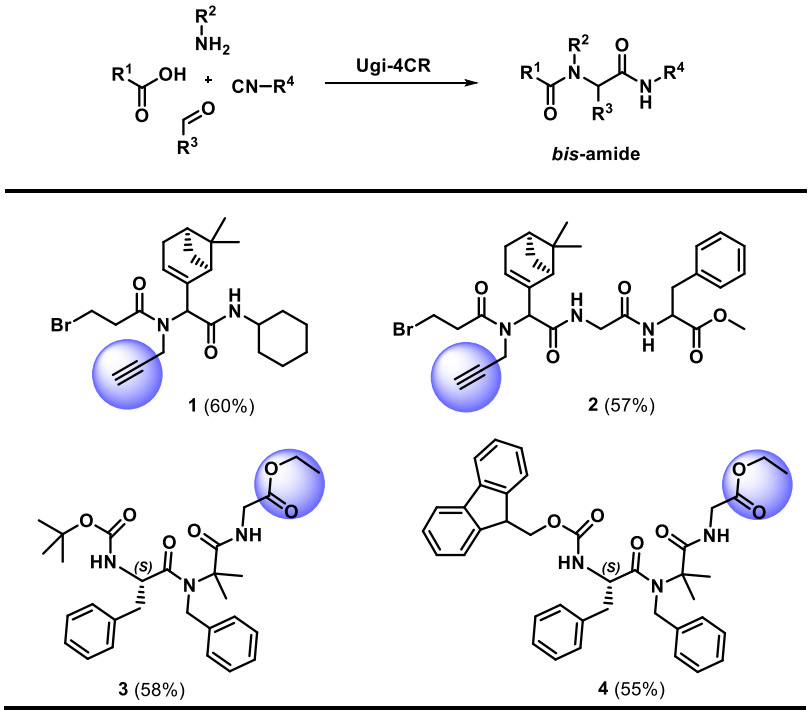

Figure 4. General synthetic scheme for the diversely functionalized peptoids (**1**–**4**).

4.09 (m, 6H), 3.98 (m, 1H), 3.89–3.65 (m, 2H), 3.28–2.84 (m, 2H), 2.33–2.05 (m, 1H), 1.51–1.37 (m, 5H), 1.29 (m, 3H), 1.25–1.19 (m, 1H). ^{13}C NMR (100 MHz, CDC_{l3}): δ 174.6, 170.8, 166.4, 161.0, 138.0, 135.6, 129.8, 129.1, 128.6, 128.0, 127.8, 127.5, 127.1, 127.0, 126.4, 126.2, 125.4, 120.3, 119.4, 119.0, 61.8, 58.8, 55.9, 45.8, 40.3, 38.7, 26.2, 25.7, 14.4 (Figure 4).

■ ASSOCIATED CONTENT

Supporting Information

The Supporting Information is available free of charge at https://pubs.acs.org/doi/10.1021/acsomega.1c02962.

NBO analysis data, dipole polarizabilities, hyperpolarizability (β_{tot}), and ^{1}H and ^{13}C NMR spectra of investigated compounds **1**, **2**, **3**, and **4** (PDF)

■ AUTHOR INFORMATION

Corresponding Authors

Muhammad Khalid − *Department of Chemistry, Khwaja Fareed University of Engineering and Information Technology, Rahim Yar Khan 64200, Pakistan;* orcid.org/0000-0002-1899-5689; Phone: +92 348 690 4807; Email: khalid@iq.usp.br, muhammad.khalid@kfueit.edu.pk

Akbar Ali − *Department of Chemistry, Government College University Faisalabad, Faisalabad 38000, Pakistan;* orcid.org/0000-0002-2914-0934; Email: akbarchm@gmail.com

Authors

Odette Concepcion − *Departamento de Química Orgánica, Facultad de Ciencias Químicas, Universidad de Concepción, Concepción 4030000, Chile*

Alexander F. de la Torre − *Departamento de Química Orgánica, Facultad de Ciencias Químicas, Universidad de Concepción, Concepción 4030000, Chile;* orcid.org/0000-0003-4767-5868

Muhammad Usman Khan − *Department of Chemistry, University of Okara, Okara 56300, Pakistan;* orcid.org/0000-0003-1900-8136

Abdul Rauf Raza − *Department of Chemistry, University of Sargodha, Sargodha 40100, Pakistan*

Ghulam Mustafa Kamal − *Department of Chemistry, Khwaja Fareed University of Engineering and Information Technology, Rahim Yar Khan 64200, Pakistan*

Muhammad Fayyaz ur Rehman − *Department of Chemistry, University of Sargodha, Sargodha 40100, Pakistan*

Mohammed Mujahid Alam − *Department of Chemistry, Faculty of Science, King Khalid University, Abha 61413, Saudi Arabia*

Muhammad Imran − *Department of Chemistry, Faculty of Science, King Khalid University, Abha 61413, Saudi Arabia*

Ataualpa Albert Carmo Braga − *Departamento de Química Fundamental, Instituto de Química, Universidade de São Paulo, São Paulo 05508-000, Brazil;* orcid.org/0000-0001-7392-3701

Mariano W. Pertino − *Institute of Natural Resources Chemistry, Universidad de Talca, Talca P.C. 3462227, Chile*

Complete contact information is available at: https://pubs.acs.org/10.1021/acsomega.1c02962

Notes

The authors declare no competing financial interest.

■ ACKNOWLEDGMENTS

A.A. gratefully acknowledges the financial support of HEC, Pakistan (project no. 21e2037/SRGP/R&D/HEC/2018). M.M.A. and M.I. express appreciation to the Deanship of Scientific Research at King Khalid University, Saudi Arabia, for funding through the research group program under grant no. R.G.P. 2/109/42. A.A.C.B. (grants 2015/01491-3 and 2014/

25770-6) is thankful to Fundacão de Amparo à Pesquisa do Estado de Sao Paulo for financial support. A.A.C.B. (grant 312550/2020-0) also thanks the Brazilian National Research Council (CNPq) for financial support and fellowships. This study was financed in part by the Coordenação de Aperfeiçoamento de Pessoal de Nivel Superior do Brasil (CAPES) Finance Code 001. A.F. de la Torre thanks FONDECYT Project No. 11200057 for the financial support. And O.C. is grateful to FONDECYT Project No. 3170012.

REFERENCES

(1) Sun, J.; Li, Z. Peptoid applications in biomedicine and nanotechnology. *Peptide Applications in Biomedicine, Biotechnology and Bioengineering*; Elsevier, 2018; pp 183−213.
(2) Ugi, I. The α-addition of immonium ions and anions to isonitriles accompanied by secondary reactions. *Angew. Chem., Int. Ed. Engl.* **1962**, *1*, 8−21.
(3) Ugi, I.; Steinbrückner, C. Isonitrile, II. Reaktion von isonitrilen mit carbonylverbindungen, aminen und stickstoffwasserstoffsäure. *Chem. Ber.* **1961**, *94*, 734−742.
(4) Peng, Z.; Yu, L. Second-order nonlinear optical polyimide with high-temperature stability. *Macromolecules* **1994**, *27*, 2638−2640.
(5) Tsutsumi, N.; Morishima, M.; Sakai, W. Nonlinear optical (NLO) polymers. 3. NLO polyimide with dipole moments aligned transverse to the imide linkage. *Macromolecules* **1998**, *31*, 7764−7769.
(6) Breitung, E. M.; Shu, C.-F.; McMahon, R. J. Thiazole and thiophene analogues of donor− acceptor stilbenes: molecular hyperpolarizabilities and structure− property relationships. *J. Am. Chem. Soc.* **2000**, *122*, 1154−1160.
(7) Ghiasuddin; Akram, M.; Adeel, M.; Khalid, M.; Tahir, M. N.; Khan, M. U.; Asghar, M. A.; Ullah, M. A.; Iqbal, M. A combined experimental and computational study of 3-bromo-5-(2, 5-difluorophenyl) pyridine and 3, 5-bis (naphthalen-1-yl) pyridine: Insight into the synthesis, spectroscopic, single crystal XRD, electronic, nonlinear optical and biological properties. *J. Mol. Struct.* **2018**, *1160*, 129−141.
(8) Ahmad, M. S.; Khalid, M.; Shaheen, M. A.; Tahir, M. N.; Khan, M. U.; Braga, A. A. C.; Shad, H. A. Synthesis and XRD, FT-IR vibrational, UV−vis, and nonlinear optical exploration of novel tetra substituted imidazole derivatives: A synergistic experimental-computational analysis. *J. Phys. Chem. Solids* **2018**, *115*, 265−276.
(9) Hussain, A.; Khan, M. U.; Ibrahim, M.; Khalid, M.; Ali, A.; Hussain, S.; Saleem, M.; Ahmad, N.; Muhammad, S.; Al-Sehemi, A. G.; Sultan, A. Structural parameters, electronic, linear and nonlinear optical exploration of thiopyrimidine derivatives: A comparison between DFT/TDDFT and experimental study. *J. Mol. Struct.* **2020**, *1201*, 127183.
(10) Shahid, M.; Salim, M.; Khalid, M.; Tahir, M. N.; Khan, M. U.; Braga, A. A. C. Synthetic, XRD, non-covalent interactions and solvent dependent nonlinear optical studies of Sulfadiazine-Ortho-Vanillin Schiff base: (E)-4-((2-hydroxy-3-methoxy-benzylidene) amino)-N-(pyrimidin-2-yl) benzene-sulfonamide. *J. Mol. Struct.* **2018**, *1161*, 66−75.
(11) Eaton, D. F. *Nonlinear Optical Materials: The Great and Near Great*; ACS Publications, 1991.
(12) Shkir, M.; Muhammad, S.; AlFaify, S.; Irfan, A.; Khan, M. A.; Al-Sehemi, A. G.; Yahia, I. S.; Singh, B.; Bdikin, I. A comparative study of key properties of glycine glycinium picrate (GGP) and glycinium picrate (GP): A combined experimental and quantum chemical approach. *J. Saudi Chem. Soc.* **2018**, *22*, 352−362.
(13) Shkir, M.; Muhammad, S.; AlFaify, S.; Irfan, A.; Patil, P. S.; Arora, M.; Algarni, H.; Jingping, Z. An investigation on the key features of a D−π−A type novel chalcone derivative for opto-electronic applications. *RSC Adv.* **2015**, *5*, 87320−87332.
(14) Muhammad, S.; Al-Sehemi, A. G.; Pannipara, M.; Irfan, A. Design, characterization and nonlinear optical properties of coumarin appended chalcones: use of a dual approach. *Optik* **2018**, *164*, 5−15.
(15) Muhammad, S.; Kumar, S.; Koh, J.; Saravanabhavan, M.; Ayub, K.; Chaudhary, M. Synthesis, characterisation, optical and nonlinear optical properties of thiazole and benzothiazole derivatives: a dual approach. *Mol. Simulat.* **2018**, *44*, 1191−1199.
(16) Khan, M. U.; Ibrahim, M.; Khalid, M.; Braga, A. A. C.; Ahmed, S.; Sultan, A. Prediction of Second-Order Nonlinear Optical Properties of D−p−A Compounds Containing Novel Fluorene Derivatives: A Promising Route to Giant Hyperpolarizabilities. *J. Cluster Sci.* **2019**, *30*, 415−430.
(17) Khan, M. U.; Ibrahim, M.; Khalid, M.; Jamil, S.; Al-Saadi, A. A.; Janjua, M. R. S. A. Quantum Chemical Designing of Indolo [3, 2, 1-jk] carbazole-based Dyes for Highly Efficient Nonlinear Optical Properties. *Chem. Phys. Lett.* **2019**, *719*, 59−66.
(18) Khalid, M.; Ullah, M. A.; Adeel, M.; Usman Khan, M.; Tahir, M. N.; Braga, A. A. C. Synthesis, crystal structure analysis, spectral IR, UV−Vis, NMR assessments, electronic and nonlinear optical properties of potent quinoline based derivatives: Interplay of experimental and DFT study. *J. Saudi Chem. Soc.* **2019**, *23*, 546−560.
(19) Ashraf, A.; Khalid, M.; Tahir, M. N.; Yaqub, M.; Naseer, M. M.; Kamal, G. M.; Saifullah, B.; Braga, A. A. C.; Shafiq, Z.; Rauf, W. A facile and concise route to (hydroxybenzoyl) pyrido [2, 3-d] pyrimidine heterocycle derivatives: synthesis, and structural, spectral and computational exploration. *RSC Adv.* **2019**, *9*, 34567−34580.
(20) Rafiq, M.; Khalid, M.; Tahir, M. N.; Ahmad, M. U.; Khan, M. U.; Naseer, M. M.; Braga, A. A. C.; Muhammad, S.; Shafiq, Z. Synthesis, XRD, spectral (IR, UV−Vis, NMR) characterization and quantum chemical exploration of benzoimidazole-based hydrazones: A synergistic experimental-computational analysis. *Appl. Organomet. Chem.* **2019**, *33*, No. e5182.
(21) Pike, N. A.; Pachter, R. Second-Order Nonlinear Optical Properties of Monolayer Transition-Metal Dichalcogenides by Computational Analysis. *J. Phys. Chem. C* **2021**, *125*, 11075.
(22) Dennington, R.; Keith, T.; Millam, J. *GaussView*, Version 5; Semichem Inc.: Shawnee Mission, KS, 2009.
(23) Frisch, M. J.; Trucks, G. W.; Schlegel, H. B.; Scuseria, G.; Robb, M. A.; Cheeseman, J. R.; Scalmani, G.; Barone, V.; Mennucci, B.; Petersson, G.; Nakatsuji, H.; Caricato, M.; Li, X.; Hratchian, H. P.; Izmaylov, A. F.; Bloino, J.; Zheng, G.; Sonnenberg, J. L.; Hada, M.; Ehara, M.; Toyota, K.; Fukuda, R.; Hasegawa, J.; Ishida, M.; Nakajima, T.; Honda, Y.; Kitao, O.; Nakai, H.; Vreven, T.; Montgomery, J. A.; Peralta, J. E.; Ogliaro, F.; Bearpark, M.; Heyd, J. J.; Brothers, E.; Kudin, K. N.; Staroverov, V. N.; Kobayashi, R.; Normand, J.; Raghavachari, K.; Rendell, A.; Burant, J. C.; Iyengar, S. S.; Tomasi, J.; Cossi, M.; Rega, N.; Millam, J. M.; Klene, M.; Knox, J. E.; Cross, J. B.; Bakken, V.; Adamo, C.; Jaramillo, J.; Gomperts, R.; Stratmann, R. E.; Yazyev, O.; Austin, A. J.; Cammi, R.; Pomelli, C.; Ochterski, J. W.; Martin, R. L.; Morokuma, K.; Zakrzewski, V. J.; Voth, G. A.; Salvador, P.; Dannenberg, J. J.; Dapprich, S.; Daniels, A. D.; Farkas, O.; Foresman, J. B.; Ortiz, J. V.; Cioslowski, J.; Fox, D. J. *D. 0109*, Revision D. 01; Gaussian Inc.: Wallingford, CT, 2009.
(24) Hanwell, M. D.; Curtis, D. E.; Lonie, D. C.; Vandermeersch, T.; Zurek, E.; Hutchison, G. R. Avogadro: an advanced semantic chemical editor, visualization, and analysis platform. *J. Cheminf.* **2012**, *4*, 17.
(25) Andrienko, G. A.; Chemcraft. *Graphical Software for Visualization of Quantum Chemistry Computations*, 2010.
(26) Khan, M. U.; Iqbal, J.; Khalid, M.; Hussain, R.; Braga, A. A. C.; Hussain, M.; Muhammad, S. Designing triazatruxene-based donor materials with promising photovoltaic parameters for organic solar cells. *RSC Adv.* **2019**, *9*, 26402−26418.
(27) Janjua, M. R. S. A.; Khan, M. U.; Khalid, M.; Ullah, N.; Kalgaonkar, R.; Alnoaimi, K.; Baqader, N.; Jamil, S. Theoretical and conceptual framework to design efficient dye-sensitized solar cells (DSSCs): molecular engineering by DFT method. *J. Cluster Sci.* **2021**, *32*, 243−253.
(28) Khan, M. U.; Khalid, M.; Arshad, M. N.; Khan, M. N.; Usman, M.; Ali, A.; Saifullah, B. Designing Star-Shaped Subphthalocyanine-Based Acceptor Materials with Promising Photovoltaic Parameters for Non-fullerene Solar Cells. *ACS Omega* **2020**, *5*, 23039−23052.

https://doi.org/10.1021/acsomega.1c02962
ACS Omega 2021, 6, 26016−26025

(29) Khan, B.; Khalid, M.; Shah, M. R.; Tahir, M. N.; Khan, M. U.; Ali, A.; Muhammad, S. Efficient Synthesis by Mono-Carboxy Methylation of 4, 4′-Biphenol, X-ray Diffraction, Spectroscopic Characterization and Computational Study of the Crystal Packing of Ethyl 2-((4′-hydroxy-[1, 1′-biphenyl]-4-yl) oxy) acetate. *ChemistrySelect* **2019**, *4*, 9274−9284.
(30) Basri, R.; Khalid, M.; Shafiq, Z.; Tahir, M. S.; Khan, M. U.; Tahir, M. N.; Naseer, M. M.; Braga, A. A. C. Exploration of Chromone-Based Thiosemicarbazone Derivatives: SC-XRD/DFT, Spectral (IR, UV−Vis) Characterization, and Quantum Chemical Analysis. *ACS Omega* **2020**, *5*, 30176−30188.
(31) Khan, I.; Khalid, M.; Adeel, M.; Khan, M. U.; Khan, M. S.; Ahmad, N.; Ali, A.; Akram, M. Palladium-catalyzed synthesis of pyrimidine substituted diaryl ethers through Suzuki Miyaura coupling reactions: Experimental and DFT studies. *Optik* **2020**, *219*, 165285.
(32) Ali, A.; Khalid, M.; Rehman, M. A.; Anwar, F.; Zain-Ul-Aabidin, H.; Akhtar, M. N.; Khan, M. U.; Braga, A. A. C.; Assiri, M. A.; Imran, M. An Experimental and Computational Exploration on the Electronic, Spectroscopic, and Reactivity Properties of Novel Halo-Functionalized Hydrazones. *ACS Omega* **2020**, *5*, 18907−18918.
(33) Khalid, M.; Ali, A.; Asim, S.; Tahir, M. N.; Khan, M. U.; Curcino Vieira, L. C.; de la Torre, A. F.; Usman, M. Persistent prevalence of supramolecular architectures of novel ultrasonically synthesized hydrazones due to hydrogen bonding [X−H···O; X= N]: Experimental and density functional theory analyses. *J. Phys. Chem. Solids* **2021**, *148*, 109679.
(34) Ali, A.; Khalid, M.; Marrugo, K. P.; Kamal, G. M.; Saleem, M.; Khan, M. U.; Concepción, O.; de la Torre, A. F. Spectroscopic and DFT/TDDFT insights of the novel phosphonate imine compounds. *J. Mol. Struct.* **2020**, *1207*, 127838.
(35) Tariq, S.; Raza, A. R.; Khalid, M.; Rubab, S. L.; Khan, M. U.; Ali, A.; Tahir, M. N.; Braga, A. A. C. Synthesis and structural analysis of novel indole derivatives by XRD, spectroscopic and DFT studies. *J. Mol. Struct.* **2020**, *1203*, 127438.
(36) Raza, A. R.; Nisar, B.; Khalid, M.; Gondal, H. Y.; Khan, M. U.; de Alcântara Morais, S. F.; Tahir, M. N.; Braga, A. A. C. A facile microwave assisted synthesis and structure elucidation of (3R)-3-alkyl-4, 1-benzoxazepine-2, 5-diones by crystallographic, spectroscopic and DFT studies. *Spectrochim. Acta, Part A* **2020**, *230*, 117995.
(37) Sultana, N.; Tariq, M. I.; Siddique, U.; Farooq, M.; Khan, M. U.; Jamil, S.; Janjua, M. R. S. A. Theoretical Investigation of Jack-in-the-Box Electro-Optical Compounds: In-Silico Design of Mixed-Argon Benzonitriles Towards the Template of Clusters. *J. Cluster Sci.* **2021**, 1−8.
(38) Khalid, M.; Lodhi, H. M.; Khan, M. U.; Imran, M. Structural parameter-modulated nonlinear optical amplitude of acceptor−π−D−π−donor-configured pyrene derivatives: a DFT approach. *RSC Adv.* **2021**, *11*, 14237−14250.
(39) Srnec, M.; Solomon, E. I. Frontier molecular orbital contributions to chlorination versus hydroxylation selectivity in the non-heme iron halogenase SyrB2. *J. Am. Chem. Soc.* **2017**, *139*, 2396−2407.
(40) Kandemirli, F.; Sagdinc, S. Theoretical study of corrosion inhibition of amides and thiosemicarbazones. *Corros. Sci.* **2007**, *49*, 2118−2130.
(41) Parr, R. G.; Szentpály, L. v.; Liu, S. Electrophilicity index. *J. Am. Chem. Soc.* **1999**, *121*, 1922−1924.
(42) Parr, R. G.; Donnelly, R. A.; Levy, M.; Palke, W. E. Electronegativity: the density functional viewpoint. *J. Chem. Phys.* **1978**, *68*, 3801−3807.
(43) Chattaraj, P. K.; Sarkar, U.; Roy, D. R. Electrophilicity index. *Chem. Rev.* **2006**, *106*, 2065−2091.
(44) Lesar, A.; Milošev, I. Density functional study of the corrosion inhibition properties of 1, 2, 4-triazole and its amino derivatives. *Chem. Phys. Lett.* **2009**, *483*, 198−203.
(45) Tahir, M. N.; Khalid, M.; Islam, A.; Ali Mashhadi, S. M.; Braga, A. A. C. Facile synthesis, single crystal analysis, and computational studies of sulfanilamide derivatives. *J. Mol. Struct.* **2017**, *1127*, 766−776.
(46) Adeel, M.; Braga, A. A. C.; Tahir, M. N.; Haq, F.; Khalid, M.; Halim, M. A. Synthesis, X-ray crystallographic, spectroscopic and computational studies of aminothiazole derivatives. *J. Mol. Struct.* **2017**, *1131*, 136−148.
(47) Khan, M. U.; Khalid, M.; Ibrahim, M.; Braga, A. A. C.; Safdar, M.; Al-Saadi, A. A.; Janjua, M. R. S. A. First Theoretical Framework of Triphenylamine−Dicyanovinylene-Based Nonlinear Optical Dyes: Structural Modification of π-Linkers. *J. Phys. Chem. C* **2018**, *122*, 4009−4018.
(48) Janjua, M. R. S. A.; Khan, M. U.; Bashir, B.; Iqbal, M. A.; Song, Y.; Naqvi, S. A. R.; Khan, Z. A. Effect of π-conjugation spacer (C C) on the first hyperpolarizabilities of polymeric chain containing polyoxometalate cluster as a side-chain pendant: A DFT study. *Comput. Theor. Chem.* **2012**, *994*, 34−40.
(49) Janjua, M. R. S. A.; Amin, M.; Ali, M.; Bashir, B.; Khan, M. U.; Iqbal, M. A.; Guan, W.; Yan, L.; Su, Z.-M. A DFT Study on The Two-Dimensional Second-Order Nonlinear Optical (NLO) Response of Terpyridine-Substituted Hexamolybdates: Physical Insight on 2D Inorganic−Organic Hybrid Functional Materials. *Eur. J. Inorg. Chem.* **2012**, *2012*, 705−711.
(50) Khan, M. U.; Ibrahim, M.; Khalid, M.; Qureshi, M. S.; Gulzar, T.; Zia, K. M.; Al-Saadi, A. A.; Janjua, M. R. S. A. First theoretical probe for efficient enhancement of nonlinear optical properties of quinacridone based compounds through various modifications. *Chem. Phys. Lett.* **2019**, *715*, 222−230.
(51) Khalid, M.; Hussain, R.; Hussain, A.; Ali, B.; Jaleel, F.; Imran, M.; Assiri, M. A.; Usman Khan, M.; Ahmed, S.; Abid, S.; Haq, S.; Saleem, K.; Majeed, S.; Jahrukh Tariq, C. Electron Donor and Acceptor Influence on the Nonlinear Optical Response of Diacetylene-Functionalized Organic Materials (DFOMs): Density Functional Theory Calculations. *Molecules* **2019**, *24*, 2096.
(52) Dömling, A.; Ugi, I. Multicomponent reactions with isocyanides. *Angew. Chem., Int. Ed.* **2000**, *39*, 3168−3210.
(53) Dömling, A. Recent developments in isocyanide based multicomponent reactions in applied chemistry. *Chem. Rev.* **2006**, *106*, 17−89.
(54) Zhang, J.; Yu, P.; Li, S.-Y.; Sun, H.; Xiang, S.-H.; Wang, J. J.; Houk, K. N.; Tan, B. Asymmetric phosphoric acid−catalyzed four-component Ugi reaction. *Science* **2018**, *361*, No. eaas8707.
(55) Sharma, U. K.; Sharma, N.; Vachhani, D. D.; Van der Eycken, E. V. Metal-mediated post-Ugi transformations for the construction of diverse heterocyclic scaffolds. *Chem. Soc. Rev.* **2015**, *44*, 1836−1860.

https://doi.org/10.1021/acsomega.1c02962
ACS Omega 2021, 6, 26016−26025